JOURNAL OF VIROLOGY, Apr. 2007, p. 3992–4001 Vol. 81, No. 8
0022-538X/07/$08.00+0 doi:10.1128/JVI.02395-06


# Inhibition of Hepatitis B Virus Polymerase by Entecavir▽

David R. Langley,* Ann W. Walsh, Carl J. Baldick, Betsy J. Eggers, Ronald E. Rose, Steven M. Levine, A. Jayne Kapur, Richard J. Colonno, and Daniel J. Tenney*

*Bristol-Myers Squibb Pharmaceutical Research Institute, Wallingford, Connecticut 06443*

Received 1 November 2006/Accepted 20 December 2006

**Entecavir (ETV; Baraclude) is a novel deoxyguanosine analog with activity against hepatitis B virus (HBV). ETV differs from the other nucleoside/tide reverse transcriptase inhibitors approved for HBV therapy, lamivudine (LVD) and adefovir (ADV), in several ways: ETV is >100-fold more potent against HBV in culture and, at concentrations below 1 μM, displays no significant activity against human immunodeficiency virus (HIV). Additionally, while LVD and ADV are obligate DNA chain terminators, ETV halts HBV DNA elongation after incorporating a few additional bases. Three-dimensional homology models of the catalytic center of the HBV reverse transcriptase (RT)-DNA-deoxynucleoside triphosphate (dNTP) complex, based on the HIV RT-DNA structure, were used with in vitro enzyme kinetic studies to examine the mechanism of action of ETV against HBV RT. A novel hydrophobic pocket in the rear of the RT dNTP binding site that accommodates the exocyclic alkene moiety of ETV was predicted, establishing a basis for the superior potency observed experimentally. HBV DNA chain termination by ETV was accomplished through disfavored energy requirements as well as steric constraints during subsequent nucleotide addition. Validation of the model was accomplished through modeling of LVD resistance substitutions, which caused an eightfold decrease in ETV susceptibility and were predicted to reduce, but not eliminate, the ETV-binding pocket, in agreement with experimental observations. ADV resistance changes did not affect the ETV docking model, also agreeing with experimental results. Overall, these studies explain the potency, mechanism, and cross-resistance profile of ETV against HBV and account for the successful treatment of naive and LVD- or ADV-experienced chronic HBV patients.**

More than 350 million people worldwide are chronically infected with hepatitis B virus (HBV), and a significant proportion of them will ultimately develop severe liver disease, including cirrhosis, hepatocellular carcinoma, and other severe complications (42). Entecavir (ETV; formerly called BMS-200475), lamivudine (LVD or 3TC; β-L-2′,3′-dideoxy-3′-thiacytidine), adefovir-dipivoxil prodrug [ADV or PMEA; 9-(2-phosphonylmethoxyethyl) adenine], and most recently, telbivudine (LdT) are oral HBV nucleoside/tide reverse transcriptase inhibitors (NRTIs) approved for the treatment of chronic HBV infection. Upon entry into the cell, all of these inhibitors require subsequent phosphorylation by cellular enzymes to generate their active moieties. The combination of intrinsic potency, exposure level, efficiency of intracellular phosphorylation, and genetic barriers to resistance all contribute to the initial and long-term efficacy of these molecules.

NRTIs inhibit the only known enzymatic target of HBV, the viral polymerase (Pol), which is characterized by several unique biological features (reviewed in reference 39). The mRNA encoding Pol serves as the template for synthesis of genomic virion DNA through reverse transcriptase (RT) activity. The RNA template is the mRNA that is translated to produce the Pol protein. The primer for Pol DNA synthesis is a hydroxyl group of a tyrosine residue near the amino terminus of Pol, resulting in covalent attachment of Pol to the progeny genome it produces. This priming is also unique in that the first three or four bases are template directed, using a stem-loop structure within the mRNA encoding Pol. The resulting primer subsequently translocates to another portion of the genome to initiate full-length first-strand DNA synthesis. Associated RNase H activity degrades the template RNA to a terminal segment of ~20 nucleotides, which itself is translocated to another region of homology to serve as the primer for second-strand DNA synthesis. The entire polymerase activity occurs within a cytoplasmic nucleocapsid particle assembled from HBV core protein, into which Pol directs the inclusion of itself and its template. The final product is a partially single-stranded, partially double-stranded gapped DNA which is released in mature virions and repaired after translocation to the nuclei of newly infected cells.

ETV triphosphate (ETV-TP) displays activity against all three synthetic activities of the HBV polymerase, i.e., the unique protein-linked priming activity, RNA-directed first-strand DNA synthesis or reverse transcription, and second-strand DNA-directed DNA synthesis (40). In addition, ETV displays higher intrinsic potency than other NRTIs in cell culture (25, 34, 50), enzymatically in vitro (40), and in clinical studies (11, 26). The low therapeutic dosage of ETV (0.5 to 1.0 mg) is primarily due to the intrinsic potency of ETV-TP against HBV RT as well as the efficiency of intracellular conversion to ETV-TP (28, 53).

While LVD, ADV, and most of the other NRTIs in development for HBV therapy are obligate terminators of DNA chain elongation because they lack a 3′-hydroxyl group required for nucleotide addition, ETV is a de facto or pseudo-terminator, halting elongation after the incorporation of a few nucleotides, presumably due to the 3′-hydroxyl moiety of its

* Corresponding author. Mailing address: Bristol-Myers Squibb Pharmaceutical Research Institute, 5 Research Parkway, Wallingford, CT 06492. Phone for David Langley: (203) 677-6656. Fax: (203) 677-7702. E-mail: david.langley@bms.com. Phone for Daniel Tenney: (203) 677-7846. Fax: (203) 677-6088. E-mail: daniel.tenney@bms.com.

▽ Published ahead of print on 31 January 2007.

cyclopentyl group (40). This is not an entirely unique property for antivirals, as the nucleoside analog penciclovir, used for treatment of herpesvirus disease, is also a de facto chain terminator.

Replacement of the methionine within the active site YMDD motif of the HBV RT with a valine or isoleucine (M204V/I) renders HBV highly resistant to LVD (LVDr) and other NRTIs containing a β-L-configured ribose isostere, such as emtricitabine (FTC), LdT, and clevudine (16, 27, 45, 46, 54). However, the presence of the LVDr substitutions M204I/V and L180M reduces viral susceptibility to ETV, a D-configured enantiomer, by a factor of eight. In contrast, HBVs with substitutions shown to encode resistance to ADV (ADVr) at RT residue position 181 or 236 retain full susceptibility to LVD and ETV (3, 23, 29, 50). Whereas single substitutions can lead to resistance to LVD and ADV, virologic rebounds due to ETVr require at least three substitutions, and ETVr variants remain susceptible to ADV (45).

Molecular modeling studies have been used to elucidate several features of human immunodeficiency virus (HIV) and HBV RTs, including the mechanisms of resistance (5, 14, 16, 24, 37). In an attempt to understand the interaction of ETV with HBV at the molecular level, we modeled ETV-TP in the catalytic site of the HBV RT as well as in elongating HBV DNA. In parallel, we performed studies of the activities of various HBV NRTIs and their corresponding triphosphates against HBV in culture and HBV RT in vitro. We also included HBV RT with substitutions creating resistance to other NRTIs in our analysis to experimentally validate modeling predictions. Our results reveal insights into the unique potency, mechanism, and cross-resistance properties of ETV.

## MATERIALS AND METHODS

**Antiviral compounds.** ETV was prepared at Bristol-Myers Squibb (BMS). The triphosphates of ETV and LdT were prepared by TriLink Biotechnologies, Inc. (San Diego, CA), ADV, LVD, LdT, tenofovir (TFV), and LVD-TP were purchased from Moravek Biochemicals (Brea, CA), and the diphosphate of ADV was prepared at BMS.

**Cells and viruses.** HepG2 human hepatoma cells, maintained in RPMI 1640 (Invitrogen, Carlsbad, CA) supplemented with 10% heat-inactivated fetal bovine serum, 100 units/ml penicillin, 100 μg/ml streptomycin, and 2 mM L-glutamine, were cultured on type I collagen-coated plastic surfaces (BD Biosciences, Bedford, MA). The laboratory clone of HBV was a genotype D *ayw* serotype clone kindly provided by Steven Goff in the plasmid pCMV-HBV (18). The plasmids containing the LVDr L180M-plus-M204V and M204I substitutions were engineered into the wild-type clone by site-directed mutagenesis. The L180M-plus-M204I-substituted plasmid was obtained from a clinical isolate.

**HBV cell culture susceptibility.** Cell culture susceptibility assays were performed by transfection of HepG2 human hepatoma cells with HBV phenotyping plasmids in the presence of a titration of antiviral agents. The level of replicated, released HBV virions was measured on day 5 through immunocapture of detergent-released nucleocapsids with anti-HBV core antibody and quantification of encapsidated HBV DNA (45). Data were plotted as percent inhibition and 50% effective concentration ($EC_{50}$) values, calculated as the drug concentration where 50% inhibition of extracellular HBV occurred.

**In vitro HBV polymerase assay.** Intracellular HBV nucleocapsids were isolated from HBV-transfected HepG2 cells and used in endogenous polymerase assays (45). The deoxynucleoside triphosphate (dNTP) $K_m$ values were determined from similar assays where the concentration of dNTPs was serially diluted from 1,000 nM to 0.3 nM. All other dNTPs were used at a fixed concentration equal to the highest test dNTP concentration, with 1/10 of the TTP in the form of [α-$^{33}$P]TTP (3,000 Ci/mmol; Perkin-Elmer, Boston, MA). The $K_m$ values were obtained from Lineweaver-Burk plots of the data generated by GraphPad Prism software, version 3.0 (San Diego, CA). The $K_i$ values were calculated using the Cheng-Prusoff equation, as follows: $K_i = IC_{50}/(1 + [S]/K_m)$ (12), where $IC_{50}$ is the 50% inhibitory concentration and $S$ is the substrate. The enzyme concentration within HBV nucleocapsid preparations was found by determining the level of covalently linked HBV DNA, using quantitative real-time PCR (28), and converting it to genome equivalents (1 pg double-stranded HBV DNA = $3 \times 10^5$ genome equivalents [22]). The primers were positioned near the 5′ end of the minus-strand DNA in an attempt to measure all enzymatically active molecules.

**Homology models of HBV RT-DNA complex.** A homology model of the wild-type HBV RT-DNA-dGTP complex was developed using the Protein Design Module in Quanta (Quanta Modeling Environment, release 2000; Accelrys Software Inc., San Diego, CA), based on the sequence alignment between HBV RT and HIV RT (16) and the HIV RT-DNA X-ray structure (Protein Data Bank accession no. 1RTD.pdb) (24). Additional HBV RT homology models were constructed with the LVDr (L180M plus M204V) and ADVr (A181T/V and N236T) substitutions. Using the DNA from the 1RTD.pdb structure as the template, different models of the DNA were constructed [d(GCXCCG GCGCTCG)-d(CGAGCGCCGG)] to model the four DNA base types and the nucleotide HBV RT inhibitors (ETV [X = C], LVD [X = G], ADV [X = T], and LdT [X = A]) bound in the dNTP binding site. Two additional DNA models were constructed with ETV modeled at the 3′ +1 and +2 positions of the newly synthesized DNA strand. The region around the dNTP binding site was equilibrated, with dGTP bound in the dNTP binding site, by running a restrained 2-nanosecond molecular dynamics (MD) simulation.

Modeling studies were conducted with Quanta (Quanta Modeling Environment, release 2000; Accelrys Software Inc., San Diego, CA) and CHARMM (8) running on a Silicon Graphics computer. The modeling figures presented were produced using DS ViewerPro 6.0 (Accelrys Software Inc., San Diego, CA). The CHARMM parameters (32) were used for all calculations carried out within the Quanta program, while the CHARMM22 (30) and CHARMM27 parameters (19) were used for the MD simulations. Switching functions were used in both energy minimization and MD simulations for the nonbonded, van der Waals, and electrostatic interactions between 8 Å and 10 Å, with a 12-Å cutoff (33, 47). The GBORN module (17) within CHARMM was used to calculate the Generalized Born salvation energy and forces. The Verlet algorithm (49) was used to calculate the classical equations of motion for the atoms, and the X-H bonds were fixed using the SHAKE algorithm (36) during MD. The following restraints were applied during all calculations: all residues with one or more atoms within 13 Å of the dGTP bound in the dNTP site were not constrained, the residues within the 13- Å to 20-Å zone from dGTP were positionally constrained with a 5-kcal harmonic tether, and all residues outside the 20-Å zone were tethered with a 50-kcal harmonic constraint. Each system was minimized with 200 steps of steepest descents followed by 500 steps of adopted-basis Newton Raphson minimization. The following MD protocol was applied to each system. In a 1.5-ps heating phase, the temperature was raised to 300 K in steps of 10 K over 0.05-ps blocks. The MD velocities were reassigned after every step, based on the Gaussian approximation, to the Maxwell Boltzmann distribution. This was followed by an equilibration phase in which the velocities were allowed to rescale over the next 18.5 ps in steps of 0.25 ps to stabilize the system within a window of 300 ± 5 K. The production phase continued for another 2 ns, where the velocities were allowed to rescale every 0.5 ps to keep the system within a window of 300 ± 10 K.

## RESULTS

The four NRTIs approved for the treatment of chronic HBV, namely, LVD, ADV, LdT, and ETV, are shown in Fig. 1A. These represent the following three structural classes with respect to the ribose isostere: L-ribose-configured nucleosides, represented by LVD and LdT; acyclic or alkyl chain isosteres administered as prodrugs of phosphonates, represented by ADV; and a novel cyclopentyl isostere, represented by ETV. Other agents that are under investigation fall into the former two categories, FTC and clevudine have an L-conformation sugar, similar to LVD and LdT (41), and TFV and other investigational agents (4) fall into the same acyclic phosphonate category as ADV. ETV is unique in having a D-configured cyclopentyl ribose isostere. All of these NRTIs must undergo intracellular conversion to the mono-, di-, and finally, active triphosphates through the action of cellular kinases or, in the

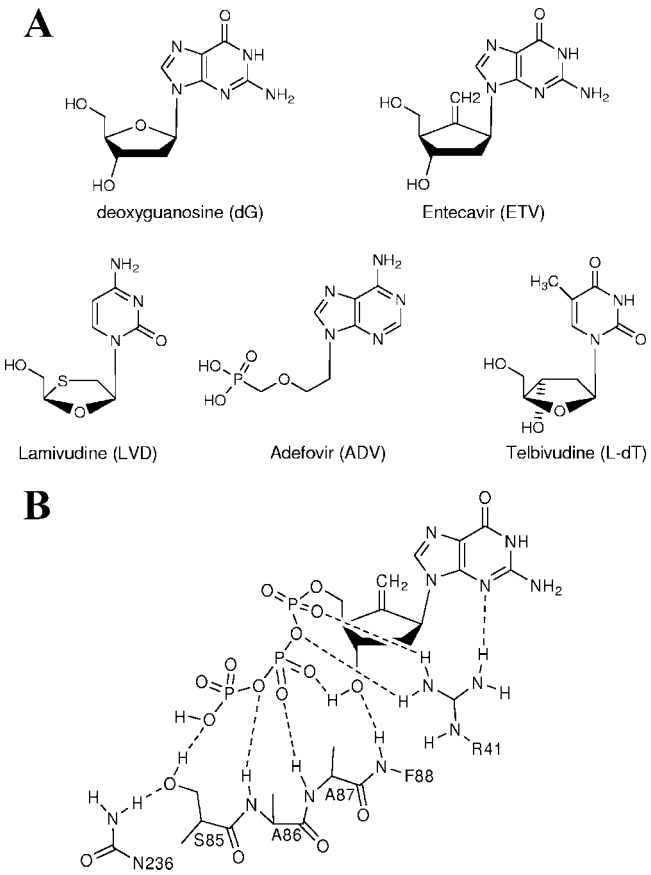


FIG. 1. ETV structure and hydrogen bonding network with HBV RT. (A) Chemical structures of deoxyguanosine, the deoxyguanosine analog ETV, the cytosine analog LVD, the adenosine monophosphonate analog ADV, and the thymidine analog LdT. (B) Hydrogen bonding network between ETV-TP and HBV RT. Note that the hydrogen bonding network between the triphosphate moiety and HBV RT is conserved for all NRTI-TPs and natural nucleotides. Only ETV and the natural nucleotides show the hydrogen bond between F88 and the 3′-hydroxyl group.

case of the phosphonate NRTIs, such as ADV and TFV, to the triphosphate analogs.

**Relative potency.** Coupled with its novel structure, ETV displayed a unique potency in HBV cell culture replication and in vitro RT enzyme assays with respect to the other HBV NRTIs (Table 1). The ETV $EC_{50}$ of a laboratory HBV isolate (18) in cell culture was 5.3 nM, making the drug 281- to 1,689-fold more potent than the other NRTIs. In an in vitro RT enzyme assay using isolated HBV nucleocapsid cores, ETV-TP displayed an $IC_{50}$ of 0.5 nM, making it >12- to 486-fold more potent than the other analogs tested. These values are consistent with the results for recombinant HBV nucleocapsids isolated from insect cells, serum-derived virions from woodchuck hepatitis virus-infected woodchucks, and duck HBV RT expressed in reticulocyte lysates (40). The potencies of NRTI triphosphates in enzyme assays can differ widely from the potencies in cell culture because the efficiency of intracellular conversion to the triphosphate plays an important role in cell culture assays. However, owing to the highly efficient conversion of ETV to ETV-TP in cells (28, 53), ETV showed superior potency in both the enzyme and culture assays (Table 1). The potency measurements were confirmed in kinetic assays, where the HBV RT inhibition constant ($K_i$) was lower than those of LVD-TP and ADV-DP. Inclusion of the relative affinity of HBV Pol for the corresponding natural dNTP is expressed in the $K_i/K_m$ ratio (Table 1). This comparison suggested that ETV-TP would compete most efficiently for the natural triphosphate in the HBV binding site.

**Molecular modeling.** To learn more about the interaction of ETV with HBV RT that results in its greater intrinsic potency, a three-dimensional homology model of HBV RT was developed based on the HIV RT-DNA crystal structure (1RTD.pdb). The most conserved domains based on the sequence alignment between HIV and HBV RTs (16) and the HIV RT-DNA X-ray structure (24) were used to build the HBV RT model. In this study, we focused our attention on the highly conserved regions surrounding the dNTP binding site. In the HBV RT–ETV-TP model, there are a number of hydrogen bonds that stabilize the complex (Fig. 1B). The γ-phosphate forms hydrogen bonds with the side chain and backbone amide NH of S85, the β-phosphate hydrogen bonds with the backbone amide NH groups of A86 and A87, and the α-phosphate hydrogen bonds with R41. Arginine 41 also hydrogen bonds with N3 of the guanine moiety, while the backbone amide NH of F88 hydrogen bonds with the 3′-hydroxyl group of the cyclopentyl isostere. The side chain conformation of S85 is further stabilized by a hydrogen bond to N236. The hydrogen-bonding network for the NRTI triphosphate moiety is conserved in all of our models for NRTIs, but only the natural nucleotides/sides and ETV-TP form the hydrogen bond between the F88 amide NH backbone and the 3′-hydroxyl moiety. Figure 2 shows the most interesting aspects of the model. In addition to the features

TABLE 1. Relative potencies of HBV NRTIs

| Drug | Culture $EC_{50}$ (nM) (mean ± SD)[a] | Difference (fold) from ETV $EC_{50}$ | Enzyme $IC_{50}$ (nM) (mean ± SD)[a,b] | Difference (fold) from ETV $IC_{50}$[b] | $K_i$ (nM)[b] | $K_m$ (nM)[b,c] | $K_i/K_m$[b] |
|---|---|---|---|---|---|---|---|
| ETV | 5.3 ± 2.5 | 1.0 | 0.5 ± 0.1 | 1 | 0.4 | 5.0 | 0.08 |
| LVD | 1,491 ± 1,033 | 281 | 6.2 ± 4.4[d] | 12.4 | 4.4 | 2.0 | 2.2 |
| ADV | 2,636 ± 1,549 | 497 | 31 ± 2.7 | 62 | 22.2 | 5.7 | 3.9 |
| LdT | 8,950 ± 4,803 | 1,689 | 243 ± 9 | 486 | — | — | — |
| TFV | 2,482 ± 1,938 | 468 | — | — | — | — | — |

[a] Values represent three or more independent experiments.
[b] —, not tested.
[c] $K_m$ values were determined with dGTP for ETV, dCTP for LVD, and dATP for ADV.
[d] LVD-TP values for this table were obtained from the work of Levine et al. (28).

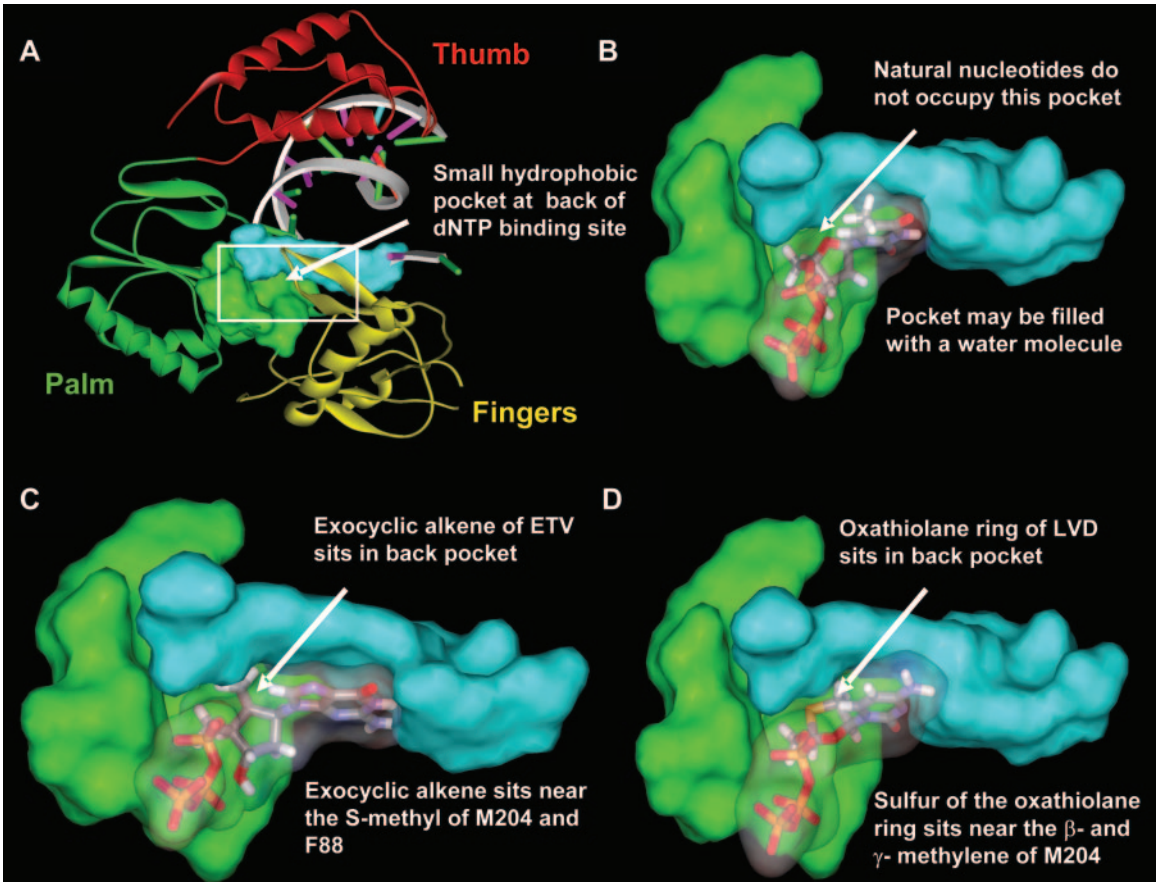


FIG. 2. (A) Homology model of HBV RT reveals a novel hydrophobic pocket at the rear of the dNTP binding site (protein, green; DNA, cyan). Natural dTTP does not access the novel pocket (B). The alkene group of the ETV cyclopentyl ribose isostere fits within the hydrophobic pocket (C). The oxathiolane ring of LVD also fits within the pocket (D).

elucidated in other HBV RT models, a small hydrophobic pocket formed at the rear of the dNTP binding site is found in the homology model of the HBV RT. The HBV RT residues that form this pocket are A87, F88, P177, L180, and M204, along with the nucleotide at the 3′ end (+1 position) of the primer DNA strand. These residues overlap but differ somewhat from those proposed by Chong et al. (14). The exocyclic double bond of ETV occupies this small pocket, forms a π-electron to *d*-orbital or donor atom-π interaction (31, 35, 44) with M204, and is proximal to the *para* position of F88. The β-L-oxathiolane ring of LVD also occupies this pocket, where the sulfur atom of the oxathiolane ring sits near the β- and γ-methylenes of M204 when bound to the HBV RT. dGTP does not occupy this pocket, thus accounting for the higher observed affinity of ETV-TP for HBV RT than that of dGTP (Table 1). LVD-TP actually exhibits an "induced fit" into this pocket, requiring some degree of distortion of the pocket to accommodate the larger β-L-oxathiolane ring of LVD-TP. This result may partially explain the lower potencies of LVD and other L-nucleosides, such as LdT and FTC, than that of ETV. The absence of this small pocket in human polymerase beta (38) correlates with the relative inactivity of ETV against this enzyme (unpublished data). Modeling of ADV-DP into the HBV RT shows that it does not access this novel pocket. When natural dNTPs and ADV-DP are bound within the dNTP binding site, this pocket is large enough and is likely occupied by a single water molecule. The binding of ETV would displace this low-affinity water molecule from the hydrophobic pocket to increase the entropy of the system. The decrease in the enthalpy of binding obtained by filling this pocket and the increase in entropy obtained by releasing the proposed trapped water would provide a relationship for the greater potency observed for ETV than for other NRTIs and the preference for ETV-TP over dGTP.

**HBV DNA chain termination.** Since ETV possesses a potential 3′-hydroxyl group, it was important to establish the effect of ETV incorporation on HBV DNA chain extension. The results of two different experiments revealed that ETV terminated HBV DNA extension and that ETV-terminated DNA was not a substrate for further elongation. First, the size of HBV DNA synthesized in cell culture was examined upon incorporation of either [$^3$H]thymidine or [$^3$H]ETV. Figure 3A shows that the size of [$^3$H]thymidine-labeled full-length HBV DNA was primarily the size expected for complete minus strands, although upon longer exposures smaller DNAs indicative of incomplete minus-strand synthesis were observed. In contrast, the size of HBV DNA that incorporated ETV was markedly smaller than the [$^3$H]thymidine-labeled full-length HBV DNA. Second, HBV nucleocapsids that were produced in cells cultured in the

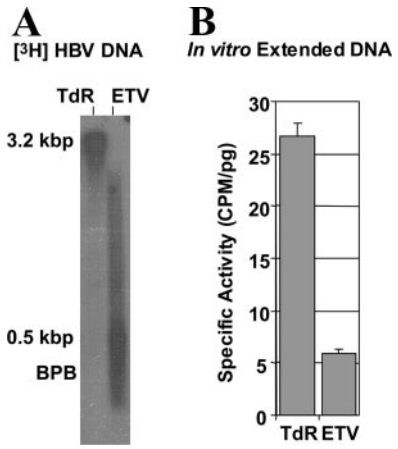


FIG. 3. HBV DNA chain termination by ETV. (A) DNAs from isolated HBV nucleocapsids after culture of cells in the presence of [$^3$H]thymidine (TdR) or [$^3$H]ETV (ETV). The migration of molecular size standards and bromphenol blue (BPB) run in parallel is indicated. (B) In vitro RT activity of nucleocapsids isolated from cells cultured with [$^3$H]thymidine or with 100 nM ETV. The incorporation of [$^{33}$P]dGTP was plotted based upon the amount of HBV DNA nucleocapsid template used to initiate the reaction. Error bars indicate the standard deviations.

presence of ETV were deficient in the ability to extend DNA chains in vitro (Fig. 3B), whereas [$^3$H]thymidine-labeled capsids were proficient in elongation. These results suggest that HBV DNA with an ETV molecule on or near the 3′ terminus is deficient in polymerase-mediated addition of nucleotides to the growing DNA.

While LVD and ADV are obligate chain terminators, lacking a 3′-hydroxyl group for nucleotide addition, ETV has a hydroxyl group for addition but displays de facto or pseudotermination after a short stretch of HBV DNA (Fig. 3) (40). The binding of ETV-TP to HBV RT occurs in an acceptable position for addition to the end of the growing HBV DNA chain (Fig. 4A), consistent with the results in Fig. 3A. Thus, the mechanism for chain termination by ETV likely involves incorporation and abortive extension of ETV-containing DNA. Modeling studies suggest that ETV chain termination can occur at several steps (Fig. 4), including (i) initial docking into the dNTP binding site and addition of ETV onto the 3′ end of the growing DNA, (ii) upon addition of a natural dNTP or ETV-TP to ETV in the +1 position, and (iii) upon further addition of nucleotides when ETV is elongated to the +2 position.

The base pairs on the growing end of the viral DNA in the HIV structure or HBV model assume an A-form conformation (24). When ETV or LVD is bound in the dNTP binding site, the exocyclic double bond of ETV or the oxathiolane ring of LVD sits in the small pocket at the back of the dNTP binding site. If the base on the 3′ end of the primer strand (+1 posi-

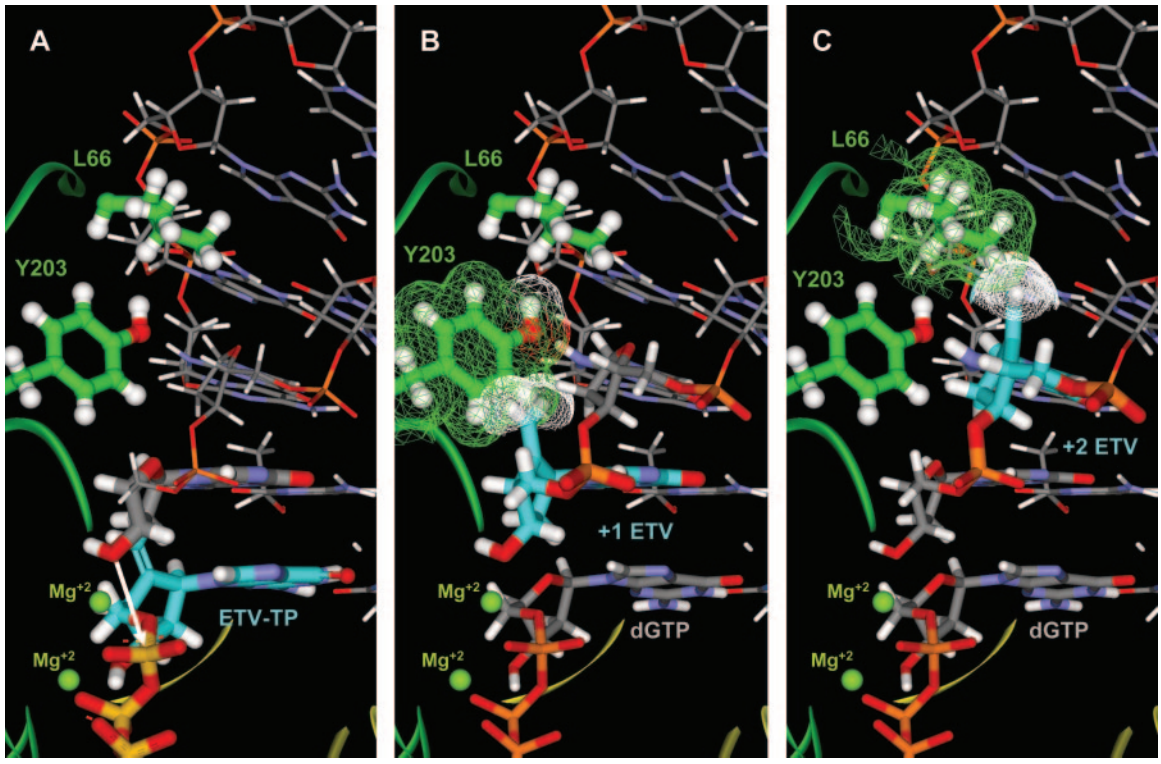


FIG. 4. Mechanism of DNA chain termination by ETV. (A) Configuration of the RT active site, primer-template DNA with dGMP in the +1 and +2 positions, $Mg^{2+}$ ions, and ETV-TP in the dNTP binding site. The arrow shows the nucleotide addition pathway. (B) ETV in the +1 position, with the steric clash between the exocyclic double bond of ETV and Y203 of HBV RT indicated (wire mesh). (C) ETV in position +2, with the steric clash between L66 of HBV RT and the alkene of ETV depicted (wire mesh). To relieve the steric strain (panels B and C), the primer distorts and the nucleotide on the 3′ end does not completely clear the dNTP binding site, sterically blocking the next dNTP from properly loading.

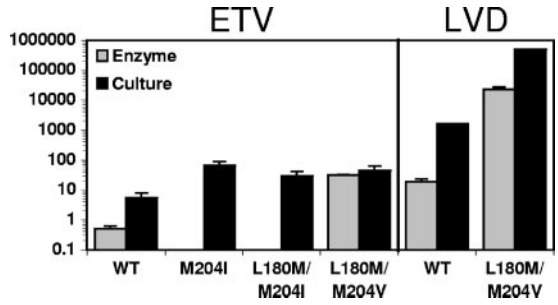


FIG. 5. Activity against LVDr HBV. The $IC_{50}$ and $EC_{50}$ values are given for NTP analogs or nucleosides/tides against HBV RT in vitro or HBV in culture, respectively, for the indicated HBV sequences. Wild-type and M204I and L180M-plus-M204V mutant clones were derived through site-directed mutagenesis of a genotype D HBV clone (18). The L180M-plus-M204I clone was derived from a patient. Values represent the means ± standard deviations for three or more independent experiments. Enzyme studies for M204I and L180M/M204I were not done.

tion) is in the southern conformation (B form), a nonreactive conformation for dNTP addition, the pocket at the back of the dNTP binding site is slightly larger and more readily accommodates either ETV or LVD. When the base on the 3′ end of the template strand is in the northern conformation (A form), the required reactive conformation for dNTP addition, the pocket at the back of the dNTP binding site is smaller and there is a slight steric hindrance between the ETV exocyclic double bond or the oxathiolane ring of LVD and the 2′-methylene of the deoxyribose ring of the DNA base in the +1 position of the growing strand (Fig. 4A). To relieve the steric hindrance, the 3′ end of the DNA slightly distorts away from the wild-type conformation (ideal conformation for dNTP addition). This distortion away from an idealized reaction path may reduce the efficiency of addition, but the distance and angle of attack remain within the reactive geometry for the SN2 reaction to occur (7, 24).

Modeling ETV into the elongating HBV DNA at the +1 position indicated that this steric congestion becomes more pronounced under these conditions. In the +1 position, the exocyclic double bond of ETV clashes with M250, Y203, and the nucleotide in the +2 position of the growing DNA chain (Fig. 4B). When ETV is modeled in the +2 position, it continues to encounter steric obstructions between the exocyclic double bond, L66, and the nucleotide in the +3 position of the growing DNA chain (Fig. 4C). To relieve the steric strain resulting from the incorporation of ETV, the DNA distorts and partially blocks the dNTP binding site, preventing its productive occupation by a new substrate, therefore resulting in chain termination.

**LVDr changes modeled into HBV RT.** LVDr is well characterized and arises through replacement of M204 within the YMDD motif of the HBV RT with isoleucine or valine, with or without the adaptive change L180M (2). The LVDr substitutions have previously been modeled into the HBV RT and proposed to result in steric hindrance of LVD-TP binding (16). HBV with LVDr substitutions displayed several thousandfold resistance to LVD in cell culture and in vitro RT studies (13, 22, 27). Figure 5 shows that LVDr HBV and LVDr RT display partial cross-resistance to ETV and ETV-TP, with approximately 8-fold and 58-fold reduced susceptibilities, respectively, consistent with previous studies (28). Despite the partial cross-resistance, ETV displayed greater potency against LVDr HBV than that of ADV or TFV. LVDr HBV having either M204I or M204V-plus-L180M substitutions also displayed very high levels of cross-resistance to LdT (45, 46, 54).

As a means to rigorously validate our HBV molecular model, we modeled HBV RT containing LVDr substitutions L180M and M204V with ETV-TP (Fig. 6). The M204 residue is part of the YMDD loop, which anchors the triphosphate of the dNTP via two $Mg^{2+}$ bridges between D205, D83, and the triphosphate moiety. Y203 of the YMDD loop also interacts with the 3′-terminal two bases of the growing DNA. In addition, both M204 and L180 form part of the pocket at the back of the dNTP binding site. The M204I or M204V substitution replaces the long flexible methionine side chain with a shorter branched side chain that results in partial filling of the small pocket at the back of the dNTP binding site that excludes the large oxathiolane moiety of LVD. This change also creates a small hole deeper within HBV RT which results in growth impairment. The compensatory L180M change partially fills the small pocket at the back of the dNTP binding site and eliminates the second hole in the protein formed by the M204 substitutions, thus restoring some efficiency to LVDr HBV RT. Figure 6 shows the changes in the pocket accessed by LVD and ETV in HBV RT as a result of LVDr changes L180M and M204V (red areas). The model predicts a steric clash between the LVDr HBV RT and LVD-TP. However, consistent with experimental results, ETV-TP can still bind the LVDr enzyme.

**ADVr changes modeled into HBV RT.** Recent studies have identified A181V/T and N236T substitutions as primary ADVr changes in HBV RT (3, 29, 50). Substitutions at A181 have also been found after virologic breakthrough during LVD (55) and famciclovir (48) therapy. In cell culture studies, the N236T (50) and A181 substitutions did not impart cross-resistance to ETV (unpublished data). Furthermore, patients failing ADV therapy with either the A181 or N236 change have shown HBV DNA reductions after switching to ETV (20). To further understand the impact that ADVr changes have on ETV susceptibility, a molecular model with ADVr changes was also constructed (Fig. 7). The A181 residue is located near the M204 *S*-methyl moiety of the YMDD loop but points away from the dNTP binding site of HBV RT (Fig. 7A). In the model, the A181V substitution results in a slight movement of the *S*-methyl moiety of M204 toward the minor groove edge of the nucleotide that is in the +1 position of the growing DNA strand. This only marginally impacts the position of the +1 nucleotide and, to a lesser extent, the YMDD loop. The N236 residue maps on the opposite end of the dNTP binding pocket, proximal to the gamma-phosphate of the dNTP. The N236 change has been proposed to reduce ADV-DP binding through a loss of hydrogen bonds and electrostatic interactions (52). In our model, N236 hydrogen bonds with S85, which in turn hydrogen bonds with the gamma-phosphate of the dNTP or NRTI (Fig. 7B). The N236T mutant loses the hydrogen bond to S85, which results in destabilization of the S85-to-gamma-phosphate interaction (52). In agreement with experimental data, there appears to be a minimal loss in interactions of ETV-TP with HBV RT containing either the A181V/T or N236T substitution. The effects of the A181V/T or N236T

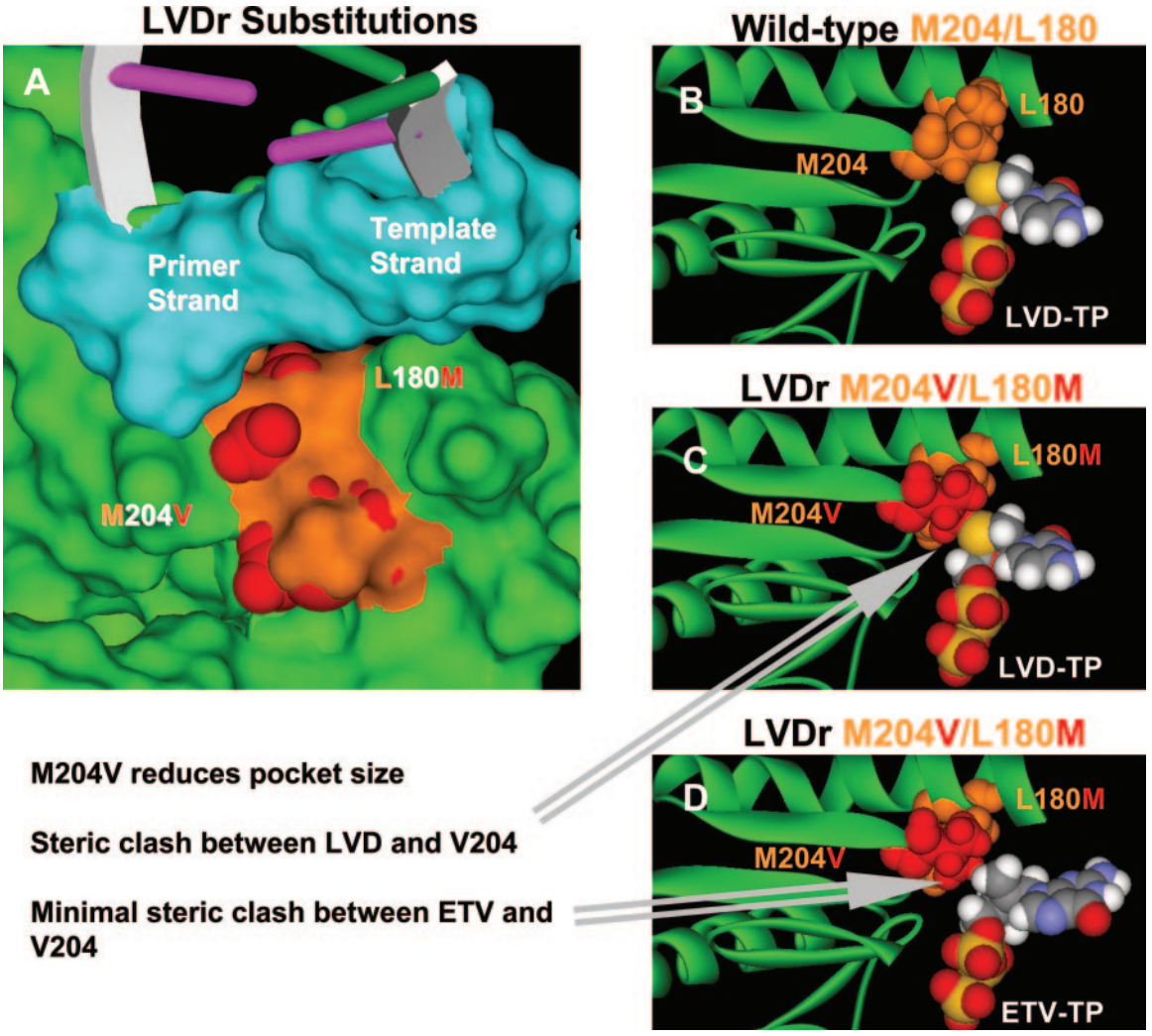


FIG. 6. HBV RT with LVDr substitutions. (A) Surface of the HBV dNTP binding site (green), with the surfaces of the wild-type M204 and L180 residues shown in orange. The van der Waals surfaces of the LVDr substitutions M204V and L180M are shown in red. The surfaces of the HBV DNA active site bases are colored turquoise, and the extended DNA is depicted as a DNA ribbon. Note that the LVDr substitutions are in the pocket shown in Fig. 2. (B, C, and D) Ribbon representations highlighting the region around the dNTP binding site and showing the YMDD loop. The van der Waals surfaces of the wild-type M204 and L180 residues are colored orange, and the van der Waals surfaces of the LVDr substitutions M204V and L180M are shown in red. (B) Favorable close contact between LVD-TP and wild-type HBV (M204 and L180). (C) Steric hindrance between LVD-TP and LVDr M204V and L180M substitutions. (D) ETV-TP does not result in steric hindrance with the LVDr M204V and L180M substitutions.

substitution are subtle but appear to have the greatest effect on the secondary stabilizing interactions that organize the dNTP binding site. The ribose isosteres of the preorganized NRTIs and natural nucleotides with lower conformational degrees of freedom, including ETV, are only marginally affected by these changes (lock and key), while the NRTIs like ADV, with conformationally flexible sugar mimics, require the more preorganized wild-type dNTP binding site (induced fit). Therefore, our model is validated in that the reported lack of cross-resistance between ADV and ETV (9, 21, 50) can be predicted.

## DISCUSSION

Since prolonged antiviral therapy can often result in the emergence of resistant virus variants, there remains a need for multiple antivirals with differing or complementary resistance patterns for effective therapy of naïve as well as treatment-experienced patients. Specific antiviral therapy for HBV includes four approved agents, LVD, ADV, LdT, and ETV, as well as several others in various stages of development. Except for ETV, these agents can be described as having either an L-configured ribose isostere or a phosphonate acyclic alkyl chain ribose isostere. ETV is unique in that it contains a cyclopentyl ribose isostere with an exocyclic alkene replacing the furanose oxygen. As such, it is considered a D-configured sugar. ETV displays several other unique features, such as subnanomolar potency against HBV RT, efficient intracellular phosphorylation, inhibition of HBV priming and first- and second-strand DNA synthesis, and nonobligate, de facto DNA chain termination. In addition, ETV has a cross-resistance profile

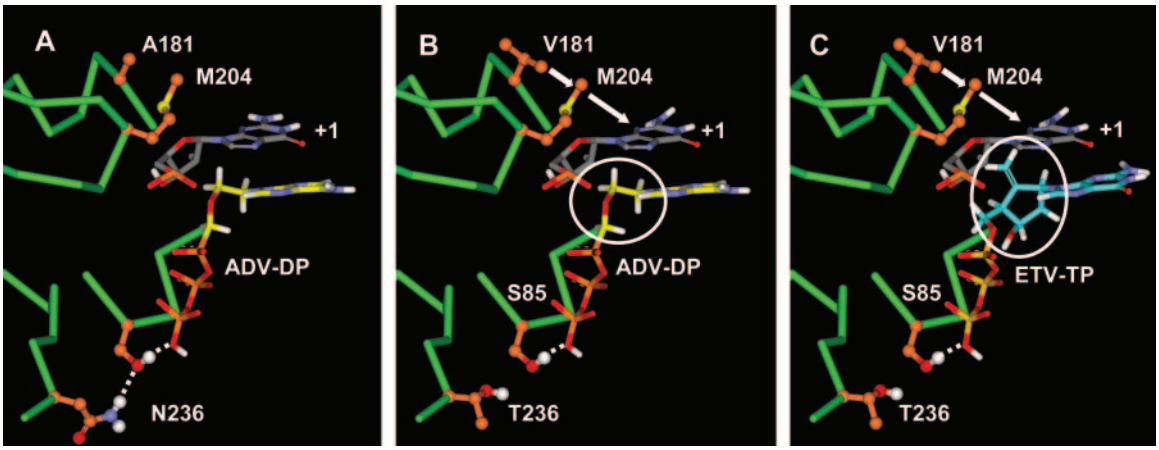


FIG. 7. Molecular model of ADVr substitutions. (A) ADV docked into the wild-type HBV RT dNTP binding site. (B) ADV docked into the ADVr HBV RT dNTP binding site. (C) ETV docked into the ADVr HBV RT dNTP binding site. Hydrogen bonds are indicated by white dotted lines. The model highlights the preorganized nature of the wild-type dNTP binding site. The ADVr mutations at N236 and A181 result in a loss of secondary stabilization. The circled moieties in panels B and C are the deoxyribose mimics in ADV and ETV, respectively. Note that the binding affinity of the flexible ADV is predictably reduced for the slightly less preorganized ADVr dNTP binding site, while binding of more rigid NRTIs, such as ETV and LVD, is not.

that is unique relative to that of the L-configured nucleoside analogs or the acyclic phosphonates. While the presence of LVDr substitutions can reduce ETV susceptibility eightfold, $IC_{50}$ and $EC_{50}$ values remain in the nanomolar range and well within the intracellular concentrations achieved with the 1-mg once-a-day dosing of ETV. Lastly, ADVr HBV retains susceptibility to ETV.

To further explore the underlying nature of ETV inhibition of HBV, we used an approach that combined cell culture and cell-free enzyme assays with molecular modeling. ETV and ETV-TP displayed higher potencies in cell culture and enzyme assays than those of all other HBV antivirals currently approved or in development, suggesting a unique interaction with the HBV RT, which we explored further using molecular modeling.

A model examining the complex of HBV RT, DNA, and dNTP was developed using the homology between the HIV RT and the HBV RT, similar to those previously described that modeled LVDr changes (5, 14, 16). The results of these ETV modeling studies were validated by enzyme analyses and suggest that the unique potency of ETV is the result of an optimal fit into a novel pocket in the rear of the dNTP binding site of HBV RT while retaining all of the key interactions of the natural nucleotide dGTP. LVD also accesses this pocket, although our model suggests that LVD must distort the pocket somewhat to achieve an "induced" fit, which may be responsible for its diminished potency relative to that of ETV. Our model confirms that LVDr substitutions result in a restriction of the pocket and a steric hindrance to binding of the oxathiolane group of LVD (16). However, the ETV alkene group can still fit into the pocket formed when LVDr substitutions are present with minimal alterations, consistent with the retention of nanomolar potency of ETV versus LVDr HBV in vitro and its clinical efficacy in LVD-refractory HBV patients (10, 43, 56). Previous investigators suggested that an antiviral with a smaller side group than the oxathiolane of LVD may retain activity against LVDr HBV (14, 16). While the fit of ETV into this pocket appears to provide the activity against both wild-type and LVDr HBV that was predicted, the high potency that ETV achieves by accessing this pocket was unpredicted.

The unique pocket into which the ETV exocyclic alkene fits in HBV RT is altered in the HIV RT structure at two positions (HBV F88/HIV Y115 and HBV L180/HIV F160). In our model, the ETV exocyclic alkene binds proximal to the hydrophobic *para* position of HBV RT F88, which is hydrophilic in HIV RT and may partially account for the reduced affinity of ETV for HIV RT. The pocket is completely absent in the structure of human cellular polymerase beta (38), likely explaining the paucity of activity against this enzyme. Studies using cellular polymerases alpha, beta, gamma, delta, and epsilon show weak or no recognition of ETV-TP (unpublished data), possibly due to an inability to accommodate ETV in the dNTP binding site.

Further validation of our HBV RT-ETV model was achieved after incorporating ADVr substitutions A181V/T and N236T. Modeling predicted that these ADVr changes should have minimal effects on the binding of HBV RT to ETV-TP. These results agree with the activity of ETV versus ADVr HBV in vitro (50) and also in patients (20). Therefore, as a result of a novel binding mechanism, ETV displays a unique cross-resistance pattern and retains the greatest potency against wild-type, LVDr, and ADVr HBVs.

LVDr substitutions that affect the positioning of the YMDD loop of HBV RT directly affect the binding of both LVD and ETV. However, a change at residue M204 (and/or L180) only accounts for partial cross-resistance to ETV. Other substitutions in RT with LVDr changes could predictably further restrict the ETV pocket and prevent binding. Indeed, some patients with prior LVDr changes at L180 and M204 displayed virologic breakthrough on ETV after additional changes in the HBV RT at positions T184, S202, and/or M250 (45, 46). These changes do not significantly affect ETV susceptibility in the absence of LVDr changes. Our initial modeling of these additional substitutions suggested that they indirectly affect ETV binding by acting in concert with the preexisting LVDr

changes, further changing the position of the YMDD loop and the size of the pocket into which ETV fits (51). However, models predicting resistance to ETV in the absence of LVDr changes involving M204 are much less plausible (unpublished data). These results are consistent with the finding that nucleoside-naïve patients treated with ETV revealed a high barrier to resistance, as reduced susceptibility to ETV was found only with at least three RT substitutions, encompassing a change at T184, S202, or M250 with the two LVDr changes M204V and L180M (15, 46).

ETV is unlike other NRTI antivirals that lack a 3′-OH and are obligate DNA chain terminators. Instead, ETV halts elongation after the addition of one or a few bases in HBV (Fig. 3) (40) or cellular polymerase genes (unpublished data). The mechanism for this chain termination was revealed by our modeling studies, which showed that incorporation of ETV into the growing DNA chain encountered a steric obstruction that progressively deteriorated the efficiency of dNTP addition with each growth step, leading to chain termination. The ultimate result, de facto or pseudo-chain termination, is similar to that for nucleoside analog inhibitors of HIV that are locked into particular conformations and terminate DNA elongation when they are unable to change conformation upon the transition from A-form to B-form DNA (6).

In summary, the combination of in vitro experiments and molecular modeling provides the mechanistic foundations for the unique potency, cross-resistance pattern, and mechanism of inhibition of ETV against HBV.

## ACKNOWLEDGMENTS

We thank BMS colleagues John Leet for providing lamivudine, Juliang Zhu for providing ADV-diphosphate, and Bruce Kreter for helpful comments on the manuscript.

## REFERENCES

1. Reference deleted.
2. **Allen, M. I., M. Deslauriers, C. W. Andrews, G. A. Tipples, K. A. Walters, D. L. Tyrrell, N. Brown, and L. D. Condreay.** 1998. Identification and characterization of mutations in hepatitis B virus resistant to lamivudine. Hepatology **27:**1670–1677.
3. **Angus, P., R. Vaughan, S. Xiong, H. Yang, W. Delaney, C. Gibbs, C. Brosgart, D. Colledge, R. Edwards, A. Ayres, A. Bartholomeusz, and S. Locarnini.** 2003. Resistance to adefovir dipivoxil therapy associated with the selection of a novel mutation in the HBV polymerase. Gastroenterology **125:**292–297.
4. **Balzarini, J., C. Pannecouque, E. De Clercq, S. Aquaro, C. F. Perno, H. Egberink, and A. Holy.** 2002. Antiretrovirus activity of a novel class of acyclic pyrimidine nucleoside phosphonates. Antimicrob. Agents Chemother. **46:** 2185–2193.
5. **Bartholomeusz, A., B. G. Tehan, and D. Chalmers.** 2004. Comparisons of the HBV and HIV polymerase, and antiviral resistance mutations. Antivir. Ther. **9:**149–160.
6. **Boyer, P., J. G. Julias, V. E. Marquez, and S. H. Hughes.** 2005. Fixed conformation nucleoside analogs effectively inhibit excision-proficient HIV-1 reverse transcriptases. J. Mol. Biol. **345:**441–450.
7. **Brautigam, C. A., and T. A. Steitz.** 1998. Structural and functional insights provided by crystal structures of DNA polymerases and their substrate complexes. Curr. Opin. Struct. Biol. **8:**54–63.
8. **Brooks, B. R., R. E. Bruccoleri, B. D. Olafson, D. J. States, S. Swaminathan, and M. Karplus.** 1983. CHARMM: a program for macromolecular energy, minimization, and dynamics calculations. J. Comput. Chem. **4:**187–217.
9. **Brunelle, M. N., A. C. Jacquard, C. Pichoud, D. Durantel, S. Carrouee-Durantel, J. P. Villeneuve, C. Trepo, and F. Zoulim.** 2005. Susceptibility to antivirals of a human HBV strain with mutations conferring resistance to both lamivudine and adefovir. Hepatology **41:**1391–1398.
10. **Chang, T., R. G. Gish, S. J. Hadziyannis, J. Cianciara, M. Rizzetto, E. R. Schiff, B. B. G. Pastore, T. Poynard, S. Joshi, K. S. Klesczewski, A. Thiry, R. E. Rose, R. J. Colonno, et al.** 2005. A dose-ranging study of the efficacy and tolerability of entecavir in lamivudine-refractory chronic hepatitis B patients. Gastroenterology **129:**1198–1209.
11. **Chang, T. T., R. G. Gish, R. de Man, A. Gadano, J. Sollano, Y. C. Chao, A. S. Lok, K. H. Han, Z. Goodman, J. Zhu, A. Cross, D. DeHertogh, R. Wilber, R. J. Colonno, D. Apelian, et al.** 2006. A comparison of entecavir and lamivudine for HBeAg-positive chronic hepatitis B. N. Engl. J. Med. **354:** 1001–1010.
12. **Cheng, Y. C., and W. H. Prusoff.** 1973. Relationship between the inhibition constant (K1) and the concentration of inhibitor which causes 50 per cent inhibition (I50) of an enzymatic reaction. Biochem. Pharmacol. **22:**3099–3108.
13. **Chin, R., T. Shaw, J. Torresi, V. Sozzi, C. Trautwein, T. Bock, M. Manns, H. Isom, P. Furman, and S. Locarnini.** 2001. In vitro susceptibilities of wild-type or drug-resistant hepatitis B virus to (−)-beta-D-2,6-diaminopurine dioxolane and 2′-fluoro-5-methyl-beta-L-arabinofuranosyluracil. Antimicrob. Agents Chemother. **45:**2495–2501.
14. **Chong, Y., L. Stuyver, M. J. Otto, R. F. Schinazi, and C. K. Chu.** 2003. Mechanism of antiviral activities of 3′-substituted L-nucleosides against 3TC-resistant HBV polymerase: a molecular modelling approach. Antivir. Chem. Chemother. **14:**309–319.
15. **Colonno, R., R. Rose, C. J. Baldick, S. Levine, K. Pokornowski, C. F. Yu, A. W. Walsh, J. Fang, M. Hsu, C. Mazzucco, B. Eggers, S. Zhang, M. Plym, K. Klesczewski, and D. J. Tenney.** 2006. Resistance after two years of entecavir treatment in nucleoside-naive patients is rare. Hepatology **44:**1656–1665.
16. **Das, K., X. Xiong, H. Yang, C. E. Westland, C. S. Gibbs, S. G. Sarafianos, and E. Arnold.** 2001. Molecular modeling and biochemical characterization reveal the mechanism of hepatitis B virus polymerase resistance to lamivudine (3TC) and emtricitabine (FTC). J. Virol. **75:**4771–4779.
17. **Dominy, B. N., and C. L. Brooks.** 1999. Development of a generalized born model parameterization for proteins and nucleic acids. J. Phys. Chem. B **103:**3765–3773.
18. **Fallows, D. A., and S. P. Goff.** 1995. Mutations in the epsilon sequences of human hepatitis B virus affect both RNA encapsidation and reverse transcription. J. Virol. **69:**3067–3073.
19. **Foloppe, N., and A. D. MacKerell.** 2000. All-atom empirical force field for nucleic acids. I. Parameter optimization based on small molecule and condensed phase macromolecular target data. J. Comput. Chem. **21:**86–104.
20. **Fung, S. K., P. Andreone, S. H. Han, K. Rajender Reddy, A. Regev, E. B. Keeffe, M. Hussain, C. Cursaro, P. Richtmyer, J. A. Marrero, and A. S. Lok.** 2005. Adefovir-resistant hepatitis B can be associated with viral rebound and hepatic decompensation. J. Hepatol. **43:**937–943.
21. **Fung, S. K., H. B. Chae, R. J. Fontana, H. Conjeevaram, J. Marrero, K. Oberhelman, M. Hussain, and A. S. Lok.** 2006. Virologic response and resistance to adefovir in patients with chronic hepatitis B. J. Hepatol. **44:** 283–290.
22. **Gaillard, R. K., J. Barnard, V. Lopez, P. Hodges, E. Bourne, L. Johnson, M. I. Allen, P. Condreay, W. H. Miller, and L. D. Condreay.** 2002. Kinetic analysis of wild-type and YMDD mutant hepatitis B virus polymerases and effects of deoxyribonucleotide concentrations on polymerase activity. Antimicrob. Agents Chemother. **46:**1005–1013.
23. **Hadziyannis, S., N. Tassopoulos, J. Heathcote, T. T. Chang, G. Kitis, et al.** 2005. Long-term therapy with adefovir dipivoxil (ADV) for HBeAg-negative chronic hepatitis B. N. Engl. J. Med. **352:**2673–2681.
24. **Huang, H., R. Chopra, G. Verdine, and S. Harrison.** 1998. Structure of a covalently trapped catalytic complex of HIV-1 reverse transcriptase; implications for drug resistance. Science **282:**1669–1675.
25. **Innaimo, S. F., M. Seifer, G. S. Bisacchi, D. N. Standring, R. Zahler, and R. J. Colonno.** 1997. Identification of BMS-200475 as a potent and selective inhibitor of hepatitis B virus. Antimicrob. Agents Chemother. **41:**1444–1448.
26. **Lai, C. L., D. Shouval, A. S. Lok, T. T. Chang, H. Cheinquer, Z. Goodman, D. DeHertogh, R. Z. R. C. Wilber, A. C. R. J. Cross, L. Fernandes, et al.** 2006. Entecavir versus lamivudine for patients with HBeAg-negative chronic hepatitis B. N. Engl. J. Med. **354:**1011–1020.
27. **Lam, W., Y. Li, J. Y. Liou, G. E. Dutschman, and Y. C. Cheng.** 2004. Reverse transcriptase activity of hepatitis B virus (HBV) DNA polymerase within core capsid: interaction with deoxynucleoside triphosphates and anti-HBV L-deoxynucleoside analog triphosphates. Mol. Pharmacol. **65:**400–406.
28. **Levine, S., D. Hernandez, G. Yamanaka, S. Zhang, R. Rose, S. Weinheimer, and R. J. Colonno.** 2002. Efficacies of entecavir against lamivudine-resistant hepatitis B virus replication and recombinant polymerases in vitro. Antimicrob. Agents Chemother. **46:**2525–2532.
29. **Locarnini, S., X. Qi, S. Arterburn, A. Snow, C. L. Brosgart, G. Currie, M. Wulfsohn, M. D. Miller, and S. Xiong.** 2005. Incidence and predictors of emergence of adefovir resistant HBV during four years of adefovir dipivoxil (ADV) therapy for patients with chronic hepatitis B (CHB). J. Hepatol. **42**(Suppl. 2)**:**17.
30. **MacKerell, A. D., D. Bashford, M. Bellott, R. L. Dunbrack, J. D. Evanseck, M. J. Field, S. Fischer, J. Gao, H. Guo, S. Ha, D. Joseph-McCarthy, L. Kuchnir, K. Kuczera, F. T. K. Lau, C. Mattos, S. Michnick, T. Ngo, D. T. Nguyen, B. Prodhom, W. E. Reiher, B. Roux, M. Schlenkrich, J. C. Smith, R. Stote, J. Straub, M. Watanabe, J. Wiorkiewicz-Kuczera, D. Yin, and M. Karplus.** 1998. All-atom empirical potential for molecular modeling and dynamics studies of proteins. J. Phys. Chem. B **102:**3586–3616.

31. **Meyer, E. A., R. K. Castellano, and F. Diederich.** 2003. Interactions with aromatic rings in chemical and biological recognition. Angew. Chem. Int. Ed. **42:**1210–1250.
32. **Momany, F. A., and R. Rone.** 1992. Validation of the general purpose QUANTA ®3.2/CHARMm® force field. J. Comput. Chem. **13:**888–900.
33. **Nilsson, L., and M. Karplus.** 1986. Empirical energy functions for energy minimization and dynamics of nucleic acids. J. Comput. Chem. **7:**591–616.
34. **Ono-Nita, S. K., N. Kato, Y. Shiratori, J. Kato, T. Goto, R. F. Schinazi, F. J. Carrilho, and M. Omata.** 2001. The polymerase L528M mutation cooperates with nucleotide binding-site mutations, increasing hepatitis B virus replication and drug resistance. J. Clin. Investig. **107:**449–455.
35. **Rotello, V. M.** 1998. The donor atom-$\pi$ interaction of sulfur with flavin. A density functional investigation. Heteroatom Chem. **9:**605–606.
36. **Ryckaert, J.-P., G. Ciccotti, and H. J. C. Berendsen.** 1977. Numerical integration of the Cartesian equations of motion of a system with constraints: molecular dynamics of n-alkanes. J. Comput. Phys. **23:**327–341.
37. **Sarafianos, S. G., K. Das, A. D. Clark, Jr., J. Ding, P. L. Boyer, S. H. Hughes, and E. Arnold.** 1999. Lamivudine (3TC) resistance in HIV-1 reverse transcriptase involves steric hindrance with beta-branched amino acids. Proc. Natl. Acad. Sci. USA **96:**10027–10032.
38. **Sawaya, M. R., R. Prasad, S. H. Wilson, J. Kraut, and H. Pelletier.** 1997. Crystal structures of human DNA polymerase beta complexed with gapped and nicked DNA: evidence for an induced fit mechanism. Biochemistry **36:**11205–11215.
39. **Seeger, C., and W. S. Mason.** 2000. Hepatitis B virus biology. Microbiol. Mol. Biol. Rev. **64:**51–68.
40. **Seifer, M., R. K. Hamatake, R. J. Colonno, and D. N. Standring.** 1998. In vitro inhibition of hepadnavirus polymerases by the triphosphates of BMS-200475 and lobucavir. Antimicrob. Agents Chemother. **42:**3200–3208.
41. **Shaw, T., A. Bartholomeusz, and S. Locarnini.** 2006. HBV drug resistance: mechanisms, detection, interpretation. J. Hepatol. **44:**593–606.
42. **Shepard, C. W., E. P. Simard, L. Finelli, A. E. Fiore, and B. P. Bell.** 2006. Hepatitis B virus infection: epidemiology and vaccination. Epidemiol. Rev. **28:**112–125.
43. **Sherman, M., C. Yurdaydin, J. Sollano, M. Silva, Y. F. Liaw, J. Cianciara, A. Boron-Kaczmarska, P. Martin, Z. Goodman, R. J. Colonno, A. Cross, G. Denisky, B. Kreter, and R. Hindes.** 2006. Entecavir for the treatment of lamivudine-refractory, HBeAg-positive chronic hepatitis B. Gastroenterology **130:**2039–2049.
44. **Singer, M. S., G. Vriend, and R. P. Bywater.** 2002. Prediction of protein residue contacts with a PDB-derived likelihood matrix. Protein Eng. **15:**721–725. doi:1093/protein/15.9.721.
45. **Tenney, D. J., S. M. Levine, R. E. Rose, A. W. Walsh, S. P. Weinheimer, L. Discotto, M. Plym, K. Pokornowski, C. Yu, P. Angus, A. Ayres, A. Bartholomeusz, W. Sievert, G. Thompson, N. Warner, S. Locarnini, and R. J. Colonno.** 2004. Clinical emergence of entecavir-resistant hepatitis B virus requires additional substitutions in virus already resistant to lamivudine. Antimicrob. Agents Chemother. **48:**3498–3507.
46. **Tenney, D. J., R. E. Rose, C. J. Baldick, S. M. Levine, K. A. Pokornowski, A. W. Walsh, J. Fang, C.-F. Yu, S. Zhang, C. M. Mazzucco, B. Eggers, M. Hsu, M. J. Plym, P. Poundstone, J. Yang, and R. J. Colonno.** 2007. Two-year assessment of entecavir resistance in lamivudine-refractory hepatitis B virus patients reveals different clinical outcomes depending on the resistance substitutions present. Antimicrob. Agents Chemother. **51:**902–911.
47. **Tidor, B., K. K. Irikura, B. R. Brooks, and M. Karplus.** 1983. Dynamics of DNA oligomers. J. Biomol. Struct. Dyn. **1:**231–252.
48. **Tillmann, H. L., C. Trautwein, T. Bock, K. H. Boker, E. Jackel, M. Glowienka, K. Oldhafer, I. Bruns, J. Gauthier, L. D. Condreay, H. R. Raab, and M. P. Manns.** 1999. Mutational pattern of hepatitis B virus on sequential therapy with famciclovir and lamivudine in patients with hepatitis B virus reinfection occurring under HBIg immunoglobulin after liver transplantation. Hepatology **30:**244–256.
49. **Verlet, L.** 1967. Computer "experiments" on classical fluids. I. Thermodynamical properties of Lennard-Jones molecules. Phys. Rev. **159:**98–103.
50. **Villeneuve, J. P., D. Durantel, S. Durantel, C. Westland, S. Xiong, C. L. Brosgart, C. S. Gibbs, P. Parvaz, B. Werle, C. Trepo, and F. Zoulim.** 2003. Selection of a hepatitis B virus strain resistant to adefovir in a liver transplantation patient. J. Hepatol. **39:**1085–1089.
51. **Walsh, A., D. Langley, R. Rose, S. Levine, K. Pokornowski, C. Yu, C. Mazzucco, M. Plym, B. Eggers, M. Hsu, C. Baldick, R. Colonno, and D. Tenney.** 2006. Mechanistic characterization of entecavir resistance in lamivudine resistant hepatitis B virus. Antivir. Res. **70:**A36.
52. **Yadav, V. C., and C. K. Chu.** 2004. Molecular mechanisms of adefovir sensitivity and resistance in HBV polymerase mutants: a molecular dynamics study. Bioorg. Med. Chem. Lett. **14:**4313–4317.
53. **Yamanaka, G., T. Wilson, S. Innaimo, G. S. Bisacchi, P. Egli, J. K. Rinehart, R. Zahler, and R. J. Colonno.** 1999. Metabolic studies on BMS-200475, a new antiviral compound active against hepatitis B virus. Antimicrob. Agents Chemother. **43:**190–193.
54. **Yang, H., C. Westland, S. Xiong, and W. E. Delaney IV.** 2004. In vitro antiviral susceptibility of full-length clinical hepatitis B virus isolates cloned with a novel expression vector. Antivir. Res. **61:**27–36.
55. **Yeh, C. T., R. N. Chien, C. M. Chu, and Y. F. Liaw.** 2000. Clearance of the original hepatitis B virus YMDD-motif mutants with emergence of distinct lamivudine-resistant mutants during prolonged lamivudine therapy. Hepatology **31:**1318–1326.
56. **Yurdaydin, C., J. Sollano, S. Hadziyannis, S. Kaymakoglu, M. Sherman, H. Brett-Smith, J. Vaughan, and R. G. Hindes.** 2006. Eighty entecavir results in continued virologic and biochemical improvement and HBeAg seroconversion through 96 weeks of treatment in lamivudine-refractory, HBeAg(+) chronic hepatitis B patients (ETV-026). J. Hepatol. **44:**S36.